

MIRKO GOJIĆ¹, LADISLAV VRŠALOVIĆ²,
STJEPAN KOŽUH¹, DIANA ČUBELA³,
SENKA GUDIĆ²

Scientific paper
UDC:620.183.6 :669.245'295

Microstructure and corrosion properties Ni-Ti alloy after electrochemical testing in 0.9 % NaCl solution

In this work the corrosion behaviour of Ni-Ti (Nitinol) shape memory alloy was studied using different electrochemical techniques including open circuit potential (E_{OC}), potentiodynamic polarization and electrochemical impedance spectroscopy (EIS). Samples made from nitinol alloy with diameter of 4 mm were used for microstructural and corrosion investigations. Testing solution was 0.9 % NaCl solution at pH=7.4, and temperature 37 ± 0.5 °C. Microstructural analysis was performed by the optical and electron scanning microscopy (SEM) equipped with energy dispersive spectrometry (EDS). High values of the oxide film resistance (R_{ox}) and the low value of corrosion current density (i_{corr}) indicated high corrosion resistance of Ni-Ti alloy, but relatively low value of breakdown potential (E_b) indicates the possibility of development localised corrosion attack on the alloy surface. Size of pits was from 10 to 100 μm and surface inclusions were initiation sites for the pitting corrosion.

Key words: nitinol, shape memory alloy, microstructure, corrosion

INTRODUCTION

Shape memory alloys (SMAs) are relatively a new class of advanced functional materials. The shape memory effect is the remembrance of the previously introduced material shape, and in physical aspect it is the consequence of martensite phase transformation in the structure of homogenous substance [1, 2]. To enable memory effect in SMA, necessary condition is presence of reversible phase transformation of austenite to martensite. Such phase transformations can be obtained by mechanical (loading) or thermal methods (cooling and heating). Numerous alloys [3-6] show shape memory effect (Ag-Cd, Au-Cd, Cu-Al-Ni, Cu-Sn, Cu-Zn, Cu-Zn-X, where X=Si, Sn, Al etc., In-Ti, Ni-Al, Ni-Ti, Fe-Pt, Mn-Cu, Fe-Mn-Si etc.). Among them the three most popular polycrystalline shape memory alloys are: Ni-Ti (nitinol), Cu-based (Cu-Zn-Al, Cu-Al-Ni etc.) and ferrous alloys (Fe-Pt, Fe-Mn-Si etc.). The Ti-Ni alloys are commonly referred as Nitinol (derived from Ni-Ti Naval Ordinance Laboratories, part of the US Department of Defence). Nitinol is the most important practical SMA for industrial and medical applications due to important shape memory effect, pseudoelasticity, corrosion resistance and biocompatibility. The most of TiNi-based alloys can be used at temperatures up to 100 °C.

The technology of production of shape memory alloys are vacuum melting, induction melting followed by vacuum arc melting, hot working (forging, rolling) followed by cold working (wire drawing, rolling). These techniques combined with heat treatments finally lead to the required products. Also is interest microtechnology for production very thin shape memory alloys such as melt-spinning or research of thin film production by vapor deposition, magnetron sputtering etc. Other processing routes productions of SMA are powder metallurgy and combustion synthesis.

Nitinol is regarded as alloy with excellent corrosion resistant, but its corrosion and electrochemical behaviour requires careful examination. The excellent corrosion resistance of NiTi results from the formation of very stable, continuous adherent and protective oxide film on its surface [7]. As titanium has high affinity for oxygen, TiO₂ based oxides form spontaneously by exposing the fresh metal surface to the air or moisture. Though NiTi is considered as corrosion resistant for general applications, its corrosion behaviour requires careful examination when is used as an implant material. If corrosion process occurs, the high nickel content of the NiTi alloys might result in potentially negative effect on surrounding tissue, like allergenicity, toxicity and carcinogenicity [8-10], due to nickel ion release.

Electrochemical investigations of the corrosion behaviour of nitinol in NaCl solution has been widely studied [11-13]. Results of these studies are different because of difference in the test methodology and quality of the surface finish. Aim of this work is the investigation of Ni-Ti alloy in 0.9 % NaCl solution

Author's address: ¹University of Zagreb, Faculty of Metallurgy, Croatia, ²University of Split, Faculty of Chemistry and Technology, Croatia, ³University of Zenica, Faculty of Metallurgy and Materials Science, Bosnia and Herzegovina

Paper received: 12. 06. 2012.

using combination of electrochemical and microstructural methods.

EXPERIMENTAL

Nitinol (49.16 at. % Ti and 49.75 at. % Ni) was casted in vacuum induction furnace in ingot (45x45x110 mm) which is annealed at 1100 °C followed cooling in water. The ingot is heated to 850 °C and hot forged into bars with different diameter (26 and 12 mm, respectively). After that the forgings are hot rolled into bars with diameter 8 and 6 mm, respectively. Samples with diameter of 4 mm were used for microstructural and corrosion investigations. For microstructural analysis before and after corrosion tests the optical and electron scanning electron microscopy (SEM) equipped with energy dispersive spectrometry (EDS) were used. For these tests Olympus GX51 and SEM Tescan Vega TS 5136 MM were used. The electrical contact for corrosion and electrochemical measurements was achieved by soldering the samples with the copper wire and then isolated with polyester, with the final exposed area of 0.125 cm². Prior to each measurements the electrode surface was polished successively with different grades of SiC paper down to 1000 grit. After that the samples were ultrasonically cleaned in ethanol and deionized water. Testing solution was 0.9 % NaCl solution at pH=7.4, and T = 37±0.5 °C.

A three electrode cell with the sample as working electrode, saturated calomel electrode (SCE) as reference electrode and platinum electrode as counter electrode were used. Corrosion behaviour of TiNi alloy was investigated by different electrochemical techniques including open circuit potential (E_{OC}), potentiodynamic polarization and electrochemical impedance spectroscopy (EIS) methods. All these measurements were performed by PAR 273A potentiostat/galvanostat and PAR M52210 lock-in amplifier for EIS measurements. An open circuit potential of the sample was continuously monitoring for 20 hours, and the potential was recorded as function of measuring time every 30 s. Potentiodynamic polarization measurements were performed in the potential range from -0.6 to 1.0 V with a scanning rate of 0.3 mV/s. The electrode was immersed in the test solution for 60 minutes prior the potentiodynamic polarization measurements. Electrochemical impedance spectroscopy tests were carried out at E_{OC} using a signal amplitude of 10 mV and a frequency interval from 0.01 Hz to 50 kHz. EIS measurements were performed after 1, 3, 6, 12 and 24 hours. The surface morphology of the NiTi samples after the potentiodynamic and EIS measurements was examined by optical and scanning electron microscopy (SEM) equipped with energy dispersive spectrometer (EDS).

RESULTS AND DISCUSSION

Figure 1 shows optical and scanning electron micrographies as well as the energy dispersive spectrum of nitinol before corrosion tests. It can be seen in Fig. 1 that surface morphology of Nitinol sample is smooth with small inclusions which are visible in the matrix alloy. According to the EDS spectrum the chemical composition of investigated shape memory alloy was 53.76 %Ni and 46.24 %Ti (wt %).

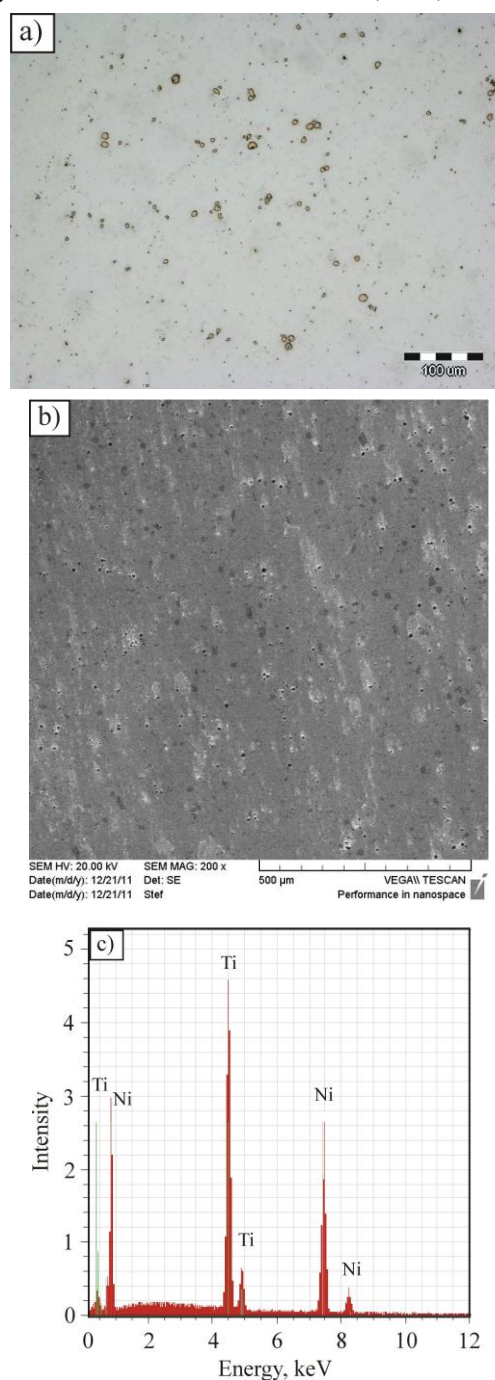


Figure 1 - Optical (a) and SEM surface morphology (b) with corresponding energy dispersive spectrum (c) of TiNi alloy before corrosion tests

The open circuit potential of the NiTi alloy was traced over the period of 20 hours of the electrode immersion in the electrolyte and the results were presented in the Fig. 2.

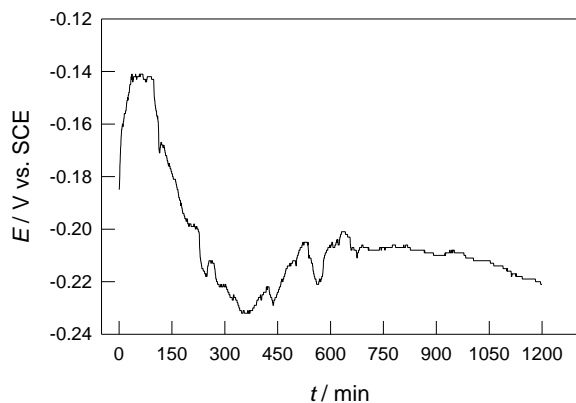


Figure 2 - Evolution of open circuit potential with time for NiTi alloy

Figure 2 shows the E_{corr} vs. time curve for the NiTi in 0.9 % NaCl solution, indicating that the corrosion process comprises two stages. The first stage lasts from the beginning to about 700 minutes is characterised by short positive change and then the sudden drop in E_{corr} values. In this stage the E_{corr} for NiTi was rather unstable with time and gradually decreased. It was believed that the decrease in E_{corr} might be caused by the formation of unstable passive film when the sample was immersed in test solution. Sudden changes in E_{corr} of NiTi occurred probably due to the formation of metastable pitting. From the literature it is known that the passive film of NiTi corroded in NaCl solution consist of mainly titanium oxides [14]. Repetitive dissolution and repair of the passive oxide film are dominant in the first stage of corrosion causing the fluctuations in E_{corr} . After immersion for a sufficiently long time, the passive oxide film covers the exposed surface and equilibrium between pitting corrosion and recovery is established, as manifested by a almost constant E_{corr} .

The representative potentiodynamic polarisation curve of the NiTi in 0.9% NaCl solution is shown in Figure 3.

The polarization curve of the NiTi is characterised by a passive region extending for about 500 mV from 0 to 450 mV. The end of the passive region represents the breakdown potential (E_b) above which the passive film breaks down and pits initiate on the surface. This is indicated by the rapid increase in the anodic current as a consequence of the passivity breakdown. The corrosion current density (i_{corr}) and corrosion potential (E_{corr}) were obtained through Tafel approximation and determined values

was: $i_{\text{corr}} = 0.40 \mu\text{A cm}^{-2}$, $E_{\text{corr}} = -0.216 \text{ V}$. Although the value of corrosion current density is low, which suggest the high corrosion resistance of investigated alloy, the passive region was relatively small, extending for about 500 mV, which indicate the susceptibility of investigated NiTi alloy to localised corrosion. This was supported with the literature findings: first, the potential value of 800 mV was established as a threshold for immunity to localized corrosion, and second, the highest potential values that titanium and its alloys can attain in vivo conditions are in the range of 450-550 mV versus SCE [15]. The pitting potential was below given potential limits which indicate the possibility of localized corrosion attack.

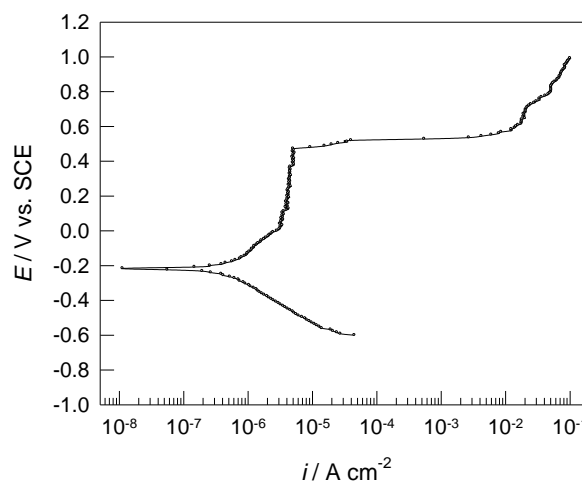


Figure 3 - Potentiodynamic polarisation curve of NiTi in 0.9% NaCl solution

In order to obtain a physical image of the system observed, impedance measurements have been performed at different stabilisation times at open circuit potential. The obtained results are presented in Figure 4 in the form of the Nyquist and Bode plots. For all stabilisation times, the shapes of impedance curves are very similar.

The response of the system in the Nyquist complex plane (Figure 4a) is a capacitive semicircle whose diameter and size increase during the first 12 hours of immersion, after which the tendency is reverse. The capacitive semicircle describes the dielectric properties of the surface oxide film.

In Bode plots at high frequencies ($f > 1 \text{ kHz}$) the data are dominated by electrolyte resistance while at very low frequencies ($f < 0.5 \text{ Hz}$) the impedance is dominated by the oxide film resistance. The phase angle drops towards 0° at both high and low frequencies. At medium frequencies the capacitive behavior of the system is evident and is determined

by the dielectric properties of the naturally formed oxide film. A slope of the Bode straight line of ≈ -1 is characteristic for this frequency range. The phase shift between current and voltage approaches a value of $\approx -90^\circ$. The high values of impedance $|Z|_{f \rightarrow 0}$ and the phase angle close to -90° are typical of a capacitive behaviour corresponding to corrosion resistant material.

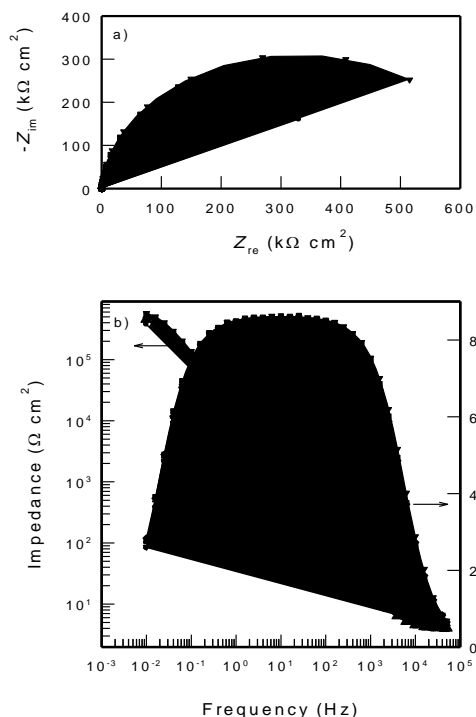


Figure 4 - Nyquist (a) and Bode (b) plots for NiTi exposed to 0.9% NaCl solution for: (●) 1 h, (▲) 3 h, (■) 6 h, (▼) 12 and (◆) 24 h

The results obtained can be described best by equivalent circuit shown in Figure 5, involving the elements R_{el} , Q and R_{ox} . In this circuit the R terms

represent resistor elements, while the Q term represent constant phase element (CPE). The constant phase element is used to describe the distribution of relaxation times, as a result of inhomogenities present at the solid/liquid interface on a microscopic level. Its impedance, Z_{CPE} , is described by expression [16]:

$$Z_{CPE} = [Q(j\omega)^n]^{-1} \quad (1)$$

where the constant Q accounts for a combination of properties related to both the surface and the electroactive species, $j\omega$ is the complex variable for sinusoidal perturbation with $\omega = 2\pi f$ and n is the exponent of CPE. The parameter n is also a constant that can assume different values in the range from -1 to $+1$. When the value of n approaches unity the CPE is equivalent to a capacitor, while n values close to 0.5 are indicative of diffusion, and consequently the CPE represents a Warburg diffusion component. Furthermore, for n values close to 0 the CPE represents the resistance and for n close to -1 , an inductance.

According to the fitting results, the n values for Q are about 0.95 . Hence, in equivalent circuit shown in Figure 5, Q is a constant phase element (CPE) accounts for the oxide film capacitances and R_{ox} is the oxide film resistance. R_{el} corresponds to the electrolyte resistance. Numerical values for each individual element of the equivalent circuit for NiTi as a function of immersion time in 0.9% NaCl solution are shown in Table 1.

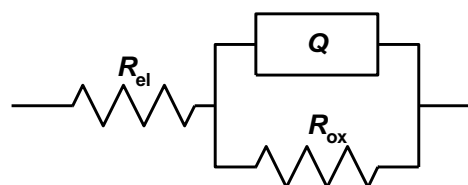


Figure 5 - Proposed equivalent circuit for NiTi in 0.9% NaCl solution

Table 1 - Equivalent circuit parameters for NiTi in 0.9% NaCl solution

Time / hours	1	3	6	12	24
$R_{el} / \Omega \text{ cm}^{-2}$	4.28	4.01	3.85	3.96	4.39
$Q \times 10^6 / \Omega^{-1} \text{ s}^n \text{ cm}^{-2}$	16.62	14.02	12.38	10.95	13.13
n	0.95	0.95	0.96	0.96	0.94
$R_{ox} / \text{k}\Omega \text{ cm}^{-2}$	420.73	537.56	623.78	659.30	585.69

It can be seen that the oxide film resistance (R_{ox}) increased, while oxide film capacity (Q) decreased with immersion time up to 12 hours. This direction of change is attributed to the increase of protective properties of the naturally formed oxide film on the NiTi electrode. Furthermore, according to the plate capacitor model the oxide film capacity, C ($n = 0.95 \pm$

0.01 ; $Q \approx C$), is inversely proportional to its thickness, d (according $C = \epsilon_0 \epsilon / d$; ϵ_0 is the permittivity of vacuum, ϵ is the relative permittivity of the film). Hence, the reduction of Q with the increase of immersion time up to 12 hours matches the corresponding increase of the thickness of the surface layer, which additionally indicated on increase of protective

properties of the oxide layer at the surface of the NiTi alloy.

After potentiodynamic and EIS measurements the rough morphology is revealed at whole alloy surface. Most of the nitinol surface area is passivated, but on one place the initiation of pitting corrosion in 0.9 % NaCl solution observed (Fig. 6). It is possible that the passive film on nitinol is breakdown due to the incorporation of chloride ions into the surface layer. It is confirmed by energy dispersive analysis of spectrums at place the initiation of pitting corrosion (Table 2).

Table 2 - Chemical composition (wt. %) from EDS spectrums of Nitinol at different sites on SEM micrography shown in Fig. 6b

Position on Fig. 6b	Ti	Ni	O	Cl
1	48.68	29.18	20.54	1.61
2	44.45	22.28	28.82	4.45
3	37.10	25.75	29.75	7.40
4	37.15	30.93	26.51	5.41
5	44.37	44.31	10.50	0.82
6	39.59	38.06	18.60	3.75

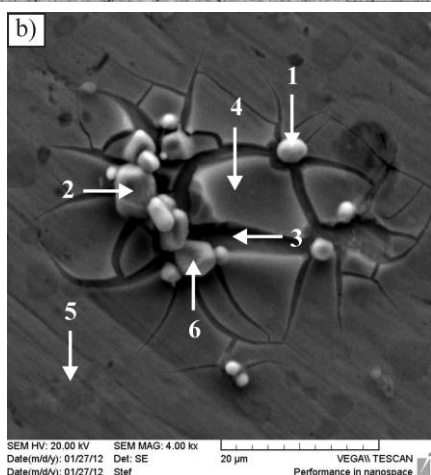
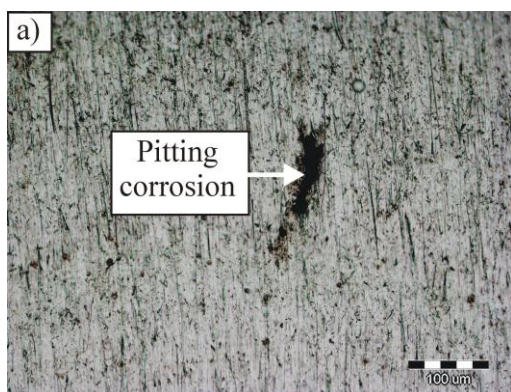


Figure 6 - Optical (a) and SEM (b) surface morphology of Nitinol after potentiodynamic testing

Our results shown in Table 2 are in agreement to studies [17] that demonstrated this passive film consists predominantly of the titanium oxide layer (TiO₂). Further careful examination by scanning electron microscopy showed the presence severe localized pitting corrosion (Figs. 7 and 8). Size of pits is from 10 to 100 μm. Inclusions affect on integrity of the passive film and they are usually initiation sites for the pitting corrosion.

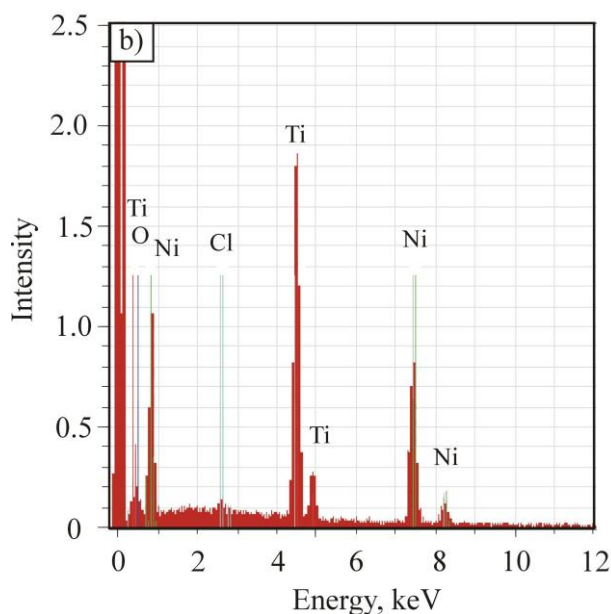
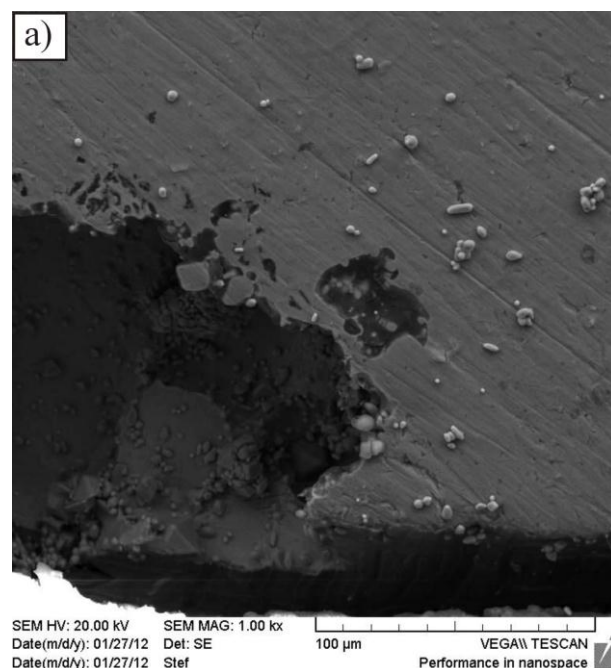


Figure 7 - SEM surface morphology (a) with corresponding EDS spectrum (b) of Nitinol after potentiodynamic polarization measurements in 0.9 % NaCl solution

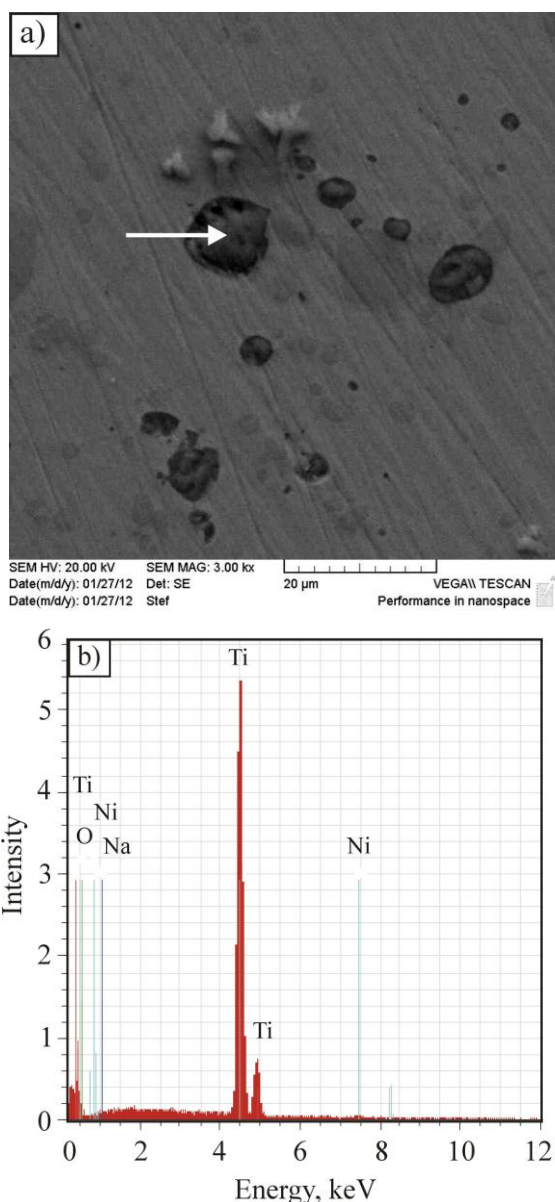


Figure 8 - SEM surface morphology (a) with corresponding EDS spectrum (b) of Nitinol after electrochemical impedance spectroscopy measurement in 0.9 % NaCl solution

The corrosion behavior of NiTi alloy greatly depends on the specific activity of the present ions, especially anions (OH^- and Cl^- ions). Namely, two processes occur simultaneously at the oxide/electrolyte interface upon stabilization of electrodes at the open circuit potential: adsorption of OH^- ions and adsorption of Cl^- ions. While, in the first place, the adsorption of OH^- ions leads to sample passivation and to improvement of the properties of the oxide film on the surface, adsorption of Cl^- ions can lead to a local dissolution of alloy. Chloride ion adsorption generally occurs at oxide defects, such as minor cuts, dips, cracks, or pores, where the oxide thickness is

smaller, and electric field is stronger. The depassivation time corresponds to time in which the amount of adsorbed aggressive ions is enough to cause nucleation of local dissolution of metallic sample. In the overall process of dissolution, the slow stage is oxide dissolution with creation of soluble salts with cations from the oxide lattice. Once when the pits were created, they continued to activate local dissolution by autocatalytic process. In the pit, there is a high concentration of metal chlorides (M^+Cl^-) and as a result of hydrolysis, a high concentration of H^+ ions. Both H^+ ions and Cl^- ions stimulate the dissolution of metal, and the entire process accelerates with time. Thus, pits propagate as a consequence of the reduction of pH within the pit [18].

It was really found out that at longer exposure times i.e. after 12 hours, there is a fall in the modulus of parameter R_{ox} and an increase of the parameter Q , while a general shape of impedance diagram is maintained (Figure 4, Table 1). This indicates the beginning of the penetration of chloride ions in the passive film.

CONCLUSION

The surface morphology of Ti-Ni (nitinol) shape memory alloy before corrosion tests was smooth with small inclusions which are visible in the matrix alloy. After electrochemical measurements of the alloy in 0.9 % NaCl solution at pH=7.4 and at temperature of 37 ± 0.5 °C by potentiodynamic polarization and electrochemical impedance spectroscopy techniques the surface morphology was changed. It was confirmed by optical microscopy, scanning electron microscopy and energy dispersive X-ray spectrometry methods. The low value of corrosion current density ($i_{corr}=0.4 \mu\text{A}/\text{cm}^2$) indicated high corrosion resistance of NiTi alloy, but relatively low value of breakdown potential (E_b) indicates the possibility of development of localised corrosion attack on the alloy surface. EIS measurements were shown that the oxide film resistance (R_{ox}) increases with increasing of time immersion up to 12 hours. The investigations of the surface morphology before electrochemical testing revealed the small inclusions in the matrix alloy which probably affect the integrity of the passive film and represent the initiation sites for the pitting corrosion. The size of pits was from 10 to 100 μm.

Note: This work was presented at XIV YuCorr International Conference "Exchanging Experiences in the Fields of Corrosions, Materials and Environmental Protection" which was maintained in April, 17-20, 2012, Tara, Serbia.

REFERENCES

- [1] M. Gojić, Alloys with the shape memory forms, *Metalurgija* (in Croatian) (1992), 31, 77-82.
- [2] K. Otsuda, X. Ren, Physical metallurgy of Ti-Ni based shape memory alloys, *Progress in Materials Science* 50 (2005) 511-678.
- [3] K. Osuka, C. M. Wayman: Shape memory alloys, Cambridge University Press, Cambridge, 1998.
- [4] D. Čorić, M. Franz: Properties and application of shape memory alloys, *Welding* (in Croatian) 50 (2007) 179-187.
- [5] W. Cai, X. L. Meng, L. C. Zhao: Recent development of TiNi-based shape memory alloys, *Solid State and Materials Science* 9 (2005) 296-302.
- [6] M. Gojić, L. Vrsalović, S. Kožuh, A. Kneissl, I. Anžel, S. Gudić, B. Kosec, M. Kliškić: Electrochemical and microstructural study of Cu-Al-Ni shape memory alloy, *Journal of Alloys and Compounds* 509 (2011) 9782-9790.
- [7] L. Tan, R.A. Dodd, W.C. Crone, Corrosion and wear-corrosion behaviour of NiTi modified by plasma source ion implementation, *Biomaterials* 24 (2003) 3931-3939.
- [8] X. Li, J. Wang, E. Han, W. Ke, Influence of fluoride and chloride on corrosion behaviour of NiTi orthodontic wires, *Acta Biomaterialia* 3 (2007) 807-815.
- [9] H.F. Hildebrand, C. Veron, P. Martin, Nickel, chromium, cobalt dental alloys and allergic reactions: an overview, *Biomaterials* 10 (1989) 545-548.
- [10] G.C. McKay, R. Macnair, C. MacDonald, M.H. Grant, Interactions of orthopaedic metals with an immortalized rat osteoblast cell line, *Biomaterials* 17 (1996) 1339-1344.
- [11] J. M. Gilemany, N. Cinca, S. Dosta, A. V. Benedetti, Corrosion behaviour of thermal sprayed nitinol coatings, *Corrosion Science* 51 (2009) 171-180.
- [12] K. T. Liu, J. G. Duh, Effect of aluminum on the corrosion behavior of NiTiAl thin films, *Applied Surface Science* 253 (2007) 5268-5273.
- [13] M. Tomita, K. Yokoyama, J. Sakai, Effect of potential, temperature and pH on hydrogen absorption and thermal desorption behaviour of Ni-Ti superelastic alloy in 0,9 % NaCl solution, Corrosion behaviour of thermal sprayed nitinol coatings, *Corrosion Science* 50 (2008) 2061-2069.
- [14] T. Hu, C.L. Chu, Y.C. Xin, S.L. Wu, K.W.K. Yeung, P.K. Chu, Corrosion products and mechanism on NiTi shape memory alloy in physiological environment, *Journal of Materials Research* 25 (2010) 350-358.
- [15] G. Rondelli, B. Vicentini, Effect of copper on the localized corrosion resistance of Ni-Ti shape memory alloy, *Biomaterials* 23 (2002) 639-644.
- [16] I.D. Raistrick, J.R. Macdonald, D.R. Franceschetti, in: J.R. Macdonald (Ed.), *Impedance Spectroscopy*, J. Wiley & Sons, New York, 1987.
- [17] X. J. Yan, D. Z. Yang, X. P. Liu, Corrosion behavior of a laser-welded NiTi shape memory alloy, *Materials Characterization* 58 (2007) 623-628.
- [18] J.R. Davis (Ed.), *Corrosion: Understanding the Basic*, ASM International, Materials Park, Ohio, 2000.

IZVOD

MIKROSTRUKTURA I KOROZIJONE OSOBINE Ni – Ti LEGURE POSLE ELEKTROHEMIJSKOG TESTA U RASTVORU 0.9% NaCl

U radu je proučavano korozijsko ponašanje Ni-Ti (Nitinol) slitine s prisjetljivosti oblika pomoću različitih elektrokemijskih metoda uključujući potencijal otvorenog strujnog kruga (E_{OC}), potenciodinamičku polarizaciju i elektrokemijsku impedancijsku spektroskopiju (EIS). Uzorci nitinola promjera 4 mm korišteni su za mikrostrukturna i korozijska ispitivanja. Otopina za ispitivanje bila je 0.9 % NaCl s $pH=7.4$ i temperaturom 37 ± 0.5 °C. Mikrostrukturna analiza je provedena optičkim i elektronskim pretražnim mikroskopom (SEM) opremljenim s energetska disperzijskim spektrometrom (EDS). Visoke vrijednosti otpora oksidnog filma (R_{ox}) i niske vrijednosti gustoće korozijske struje (i_{corr}) upućuju na visoku korozijsku otpornost Ni-Ti slitine, ali relativno niska vrijednost potencijala pucanja filma (E_b) upućuju na mogućnost razvoja lokalnog korozijskog napada na površini slitine. Veličina jamice je bila od 10 do 100 μm , dok su uključci bili inicijalna mjesta za jamičastu koroziju.

Ključne riječi: nitinol, slitine s prisjetljivosti oblika, mikrostruktura, korozija

Rad primljn: 12.06.2012.

Originalni naučni rad

Rad je saopšten na Y'UCORR'12